RESEARCH PAPER

PCCP
www.rsc.org/pccp

Chain-length-dependent conformational transformation and melting behaviour of alkyl/oligo(oxyethylene)/alkyl triblock compounds: α-octyl-ω-octyloxyoligo(oxyethylene)s

Koichi Fukuhara,*[a] Takahiro Mizawa,[a] Tomohiro Inoue,[a] Hirotaka Kumamoto,[a] Yoshihide Terai,[a] Hiroatsu Matsuura[a] and Kyriakos Viras[ab]

[a] *Department of Chemistry, Graduate School of Science, Hiroshima University, Kagamiyama, Higashi-Hiroshima, 739-8526, Japan. E-mail: kfuku@sci.hiroshima-u.ac.jp; Fax: +81-82-424-0727*

[b] *Department of Chemistry, National and Kapodistrian University of Athens, Panepistimiopolis, Athens, 157 71, Greece*

Received 17th September 2004, Accepted 1st February 2005
First published as an Advance Article on the web 21st February 2005

The chain-length-dependent conformational transformation and the melting behaviour of triblock compounds α-octyl-ω-octyloxyoligo(oxyethylene)s, $H(CH_2)_8(OCH_2CH_2)_mO(CH_2)_8H$ (abbreviated as $C_8E_mC_8$) (m = 1–8), have been studied by infrared spectroscopy and differential scanning calorimetry. The compounds with m = 1–5 assume the all-*trans* planar form (γ-form) in the solid state, while those with m = 7 and 8 assume the planar/helical/planar form with conformational defects in the alkyl chain (β′-form). Conformational polymorphism was observed for $C_8E_6C_8$: the γ-form for the annealed solid and the planar/helical/planar form without conformational defects (β-form) for the unannealed solid. The conformational transformation from the planar form into the planar/helical/planar form takes place at a length of the oligo(oxyethylene) chain m = 6. This result for $C_8E_mC_8$ and a similar conformational transformation for $C_6E_mC_6$ at m = 5 (previous work) demonstrate that the conformation of the $C_nE_mC_n$ triblock compounds in the solid state is determined by intramolecular conformational restoring force in the central oligo(oxyethylene) block, intermolecular dipole–dipole interaction of the C–O bonds and intermolecular packing force in the end alkyl blocks. The melting points of the γ-form solid of $C_8E_mC_8$ are much lower than the melting points of *n*-alkanes with similar molecular masses. The observed thermodynamic quantities show that the planar structure of the oligo(oxyethylene) chain is stabilized by the force of the magnitude that maintains the rotator phase of *n*-alkanes. For the β′-form solid of $C_8E_mC_8$, the alkyl blocks, which are partially noncrystalline, and the oligo(oxyethylene) block melt together at the melting point, unlike the β-form solid of $C_6E_mC_6$, for which the melting of the alkyl blocks takes place before the melting of the oligo(oxyethylene) block. The β-form solid of $C_8E_6C_8$ (unannealed) melts *via* the γ-form solid.

1. Introduction

Aggregate structures of block copolymers consisting of chemical blocks that tend to crystallize are strongly affected by the lengths of the constituent blocks, since the crystallization of one block influences the crystallization of other blocks.[1] The higher-order structures formed by these copolymers have attracted much attention in the field of soft materials science as a new design for mesoscopic structures.[2–5] The typical examples are chain compounds that comprise the blocks of different conformational natures, *i.e.*, those block compounds consisting of *n*-alkyl chain $(–CH_2–)_n$, which prefers the extended zigzag structure with all-*trans* conformation,[6] and oligo(oxyethylene) chain $(–OCH_2CH_2–)_m$, which prefers the helical structure with a repeated *trans–gauche–trans* conformation for the $O–CH_2–CH_2–O$ segment.[7]

Booth and co-workers[8,9] have revealed, using differential scanning calorimetry (DSC), X-ray scattering and infrared and Raman spectroscopy, that several solid structures with different crystallinity exist for alkyl/oligo(oxyethylene)/alkyl triblock compounds $H(CH_2)_n(OCH_2CH_2)_mO(CH_2)_nH$ (abbreviated as $C_nE_mC_n$) with n = 1–26 and m = 9 and 15. They classified the structures of these compounds on the basis of the crystallinity of the constituent blocks; structure I is characterized by a noncrystalline alkyl block and crystalline oligo(oxyethylene) block, structure II is characterized by crystalline alkyl and oligo(oxyethylene) blocks and structure III is characterized by a crystalline alkyl block and noncrystalline oligo(oxyethylene) block. With increasing n, the structure of the $C_nE_mC_n$ homologues changes from structure I to III *via* II. These structural changes were explained by the preclusion of crystallization of the minor block by the major block.

For short-chain symmetric $C_nE_mC_n$ triblocks (n = 3–8, 10 and m = 1–8)[10–13] and asymmetric triblocks $H(CH_2)_n(OCH_2CH_2)_mO(CH_2)_{n'}H$ ($C_nE_mC_{n'}$) (n = 8, n' = 2–7 and m = 4),[14] we have obtained the following results: both the alkyl and oligo(oxyethylene) blocks are crystalline, a highly extended all-*trans* planar form and a planar/helical/planar form exist, and the chain-length-dependent conformational transformation and polymorphism occur. The same experimental results have been reported by Rabolt and co-workers.[15] The all-*trans* planar form, called the γ-form, has been observed for the $C_nE_mC_{n'}$ compounds with end alkyl blocks having the length comparable to or longer than that of the central oligo(oxyethylene) block (*i.e.*, $n + n' \gtrsim 3m$).[12] In the γ-form, the oligo(oxyethylene) chain is constrained to assume a planar structure with the all-*trans* conformation. The planar/helical/planar form, on the other hand, has been observed for $C_nE_mC_{n'}$ with end alkyl blocks having the length shorter than that of the central oligo(oxyethylene) block. This latter form is subclassified into two, the β-form and the αβ-form.[10–14] The difference between the two forms lies in the conformation around the CC–CO

DOI: 10.1039/b414340j

bonds on both sides of the central oligo(oxyethylene) block; the β-form assumes the *gauche* conformation around two of these bonds, while the αβ-form assumes the *trans* conformation around one of them and the *gauche* conformation around the other. It has also been shown that the alkyl block of some of symmetric $C_nE_mC_n$ with $n \lesssim m$ is partially crystalline or noncrystalline and contains conformational defects such as end-*gauche* and kink, while the oligo(oxyethylene) block is crystalline with normal helical conformation.[13]

The chain-length-dependent conformational transformation of $C_nE_mC_n$ from the all-*trans* planar form into the planar/helical/planar form or the transformation *vice versa* has been attributed to a crystallization competition between the oligo(oxyethylene) and alkyl blocks, and the unusual planar structure of the oligo(oxyethylene) block has been interpreted as a result from the conformational adaptation of this block to the restricted lattice space formed by the alkyl blocks.[13] Our recent thermal and infrared spectroscopic study on $C_6E_mC_6$ ($m = 1$–7) with high purity (>99.7%) has shown the relationship between the molecular conformation and the thermal behaviour, which depend on the number of oxyethylene units.[16] The relevant results are as follows: (1) the melting points of the γ-form $C_nE_mC_n$ are significantly lower than those of the corresponding *n*-alkanes despite the same molecular form; (2) the planar structure of the central oligo(oxyethylene) chain in the γ-form is stabilized by the force of the magnitude that maintains the rotator phase of *n*-alkanes; (3) the melting points of the γ-form $C_6E_mC_6$ exhibit the odd–even alternation with respect to the number of oxyethylene units (*m*); (4) the β-form $C_6E_mC_6$ melt *via* a partially melted phase where the alkyl blocks are melted; and (5) conformational polymorphism takes place for $C_6E_5C_6$ depending on solidification conditions.

In the present work, we have extended the conformational and thermal studies of triblock compounds to $C_8E_mC_8$ ($m =$ 1–8), the compounds with longer alkyl chains than in $C_6E_mC_6$,[16] aiming at acquiring a comprehensive understanding of chain-length-dependent conformational transformation and melting behaviour of alkyl/oligo(oxyethylene)/alkyl triblock compounds. We used the samples of $C_8E_mC_8$ with high purity of 99.49–99.96% to perform precise measurements of infrared spectroscopy and DSC. This purity is much higher than the purity (95–99%) of the same compounds used for the previous studies.[11,13]

2. Experimental

2.1. Materials

$C_8E_mC_8$ with $m = 1$–4 were prepared from 1-chlorooctane and mono-, di-, tri- and tetraethylene glycols, respectively, with tetrabutylammonium hydrogensulfate as a phase transfer catalyst.[17] $C_8E_mC_8$ with $m = 5$–8 were prepared with use of the same catalyst from 1-chloro-3,6-dioxatetradecane and mono-, di-, tri- and tetraethylene glycols, respectively. The products were purified by repeated vacuum distillations and Kugelrohr distillation. Some of the $C_8E_mC_8$ were purified by column chromatography on silica gel prior to the distillation. The purity was checked by gas chromatography to be 99.96% for $C_8E_1C_8$, 99.96% for $C_8E_2C_8$, 99.79% for $C_8E_3C_8$, 99.86% for $C_8E_4C_8$, 99.72% for $C_8E_5C_8$, 99.79% for $C_8E_6C_8$, 99.49% for $C_8E_7C_8$ and 99.68% for $C_8E_8C_8$.

2.2. Infrared measurements

The infrared spectra of $C_8E_mC_8$ ($m = 1$–8) were recorded on a Perkin–Elmer Spectrum One Fourier transform spectrometer with a spectral resolution of 2.0 cm^{-1}. The spectrometer was purged with dry nitrogen gas before the measurements. A Peltier cryostat cell was used to measure the infrared spectra in the solid state in a temperature range from 240 to 300 K. The infrared spectra were also measured at 100 K by cooling with liquid nitrogen. In these measurements, the liquid samples at room temperature were placed between KRS-5 plates and were cooled to obtain the solid.

2.3. DSC measurements

The DSC melting curves of $C_8E_mC_8$ ($m = 1$–8) were measured on a Shimadzu DSC-50 differential scanning calorimeter equipped with a Shimadzu LTC-50 cooling jacket. The thermodynamic quantities, *i.e.*, melting point, solid–solid transition temperature, enthalpy of melting and enthalpy of solid–solid transition, were measured at a rate of heating of 3.0 K min^{-1} over a temperature range from 240 to 300 K. This rate of heating was adopted as standard in this work. Measurements with different rates of heating, *i.e.*, 0.3, 10.0 and 20.0 K min^{-1}, were also performed to examine the possible effect of the scan rate on DSC curves. Prior to the measurements, the samples were solidified at a rate of cooling of 3.0 K min^{-1} and were kept at about 230 K for 30 min. Annealing was applied to the solidified samples to examine the thermal-history dependency of the DSC curves. The temperature and the enthalpy change were calibrated by using the standard samples, *n*-dodecane, *n*-hexadecane and indium. The reproducibility of the observed DSC melting curves was confirmed by the measurements on different samples of the same compound.

3. Calculations

Normal coordinate calculations were performed on the possible conformational forms of all $C_8E_mC_8$ compounds studied after examining the pertinent conformation key bands of the alkyl[18,19] and oligo(oxyethylene) chains.[20] The computation was carried out with the program MVIB[21] on Windows. The calculations yielded detailed information on the normal modes of vibrations that are sensitive to the local conformation of the alkyl and oligo(oxyethylene) chains.

4. Results and discussion

4.1. Molecular conformation

The infrared spectra of $C_8E_mC_8$ ($m = 1$–8) measured at 240 K are shown in Fig. 1, where the wavenumbers of the conformation key bands are indicated. The spectra at 100 K are substantially the same as those at 240 K. Of the $C_8E_mC_8$ studied, only $C_8E_6C_8$ gave two different spectra depending on thermal history; namely, the spectrum of the solid obtained by annealing the once solidified substance and the spectrum of the solid obtained without annealing are different. In our previous study on $C_8E_mC_8$ ($m = 6$–8) with lower purity (95–99%),[13] we found that $C_8E_7C_8$, in addition to $C_8E_6C_8$, gave two different infrared spectra at liquid nitrogen temperature, depending on thermal history. The spectrum of $C_8E_7C_8$ in this work is the same as the previous spectrum obtained by rapid cooling (no annealing).[13] We have attempted to reproduce the other spectrum of $C_8E_7C_8$ observed in the previous work, but we could not obtain the relevant spectrum on any condition due most probably to the difference in the sample purity.

The infrared spectra of $C_8E_mC_8$ (Fig. 1) can be classified into two types, A and B, according to their characteristic features.[13] The spectra of $C_8E_1C_8$–$C_8E_5C_8$ and $C_8E_6C_8$ (annealed) are of type A. This type is characterized by a distinct band at 1500–1490 cm^{-1}, a strong band at about 965 cm^{-1} and a few weak bands in the 600–500 cm^{-1} region (not shown in the figure). These spectral features are the characteristics of the γ-form triblocks.[13] The normal coordinate calculations confirm that all of the bands in the type-A spectra are in agreement with the results for the fully extended γ-form. The spectra of $C_8E_6C_8$ (unannealed), $C_8E_7C_8$ and $C_8E_8C_8$, on the other hand, are of type B. This type is characterized by a well-defined band at about 1280 cm^{-1}, strong bands centered around 1115 cm^{-1}

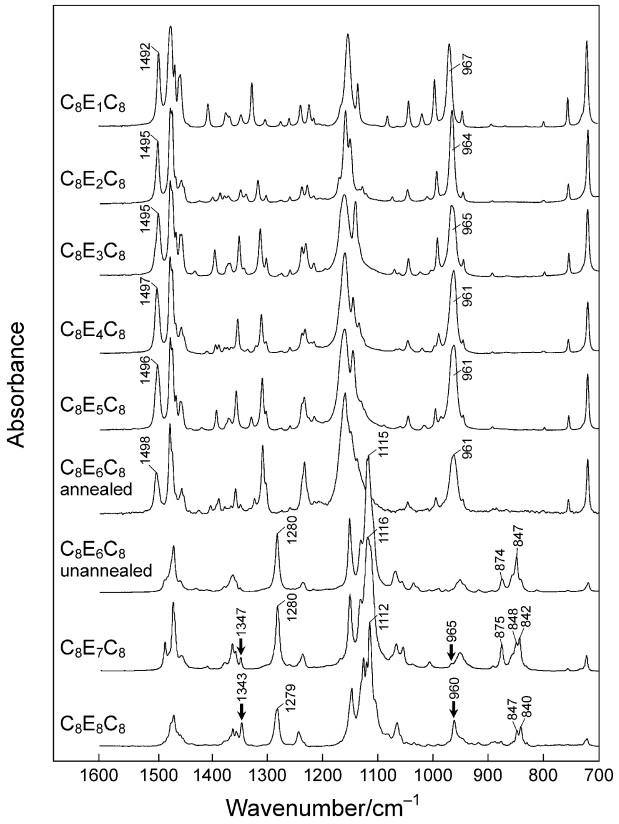

Fig. 1 Infrared spectra of $C_8E_mC_8$ (m = 1–8) at 240 K. The wavenumbers of the conformation key bands are indicated in the figure.

and a complex spectral feature in the 900–800 cm^{-1} region. These characteristic bands have been assigned to the *trans–gauche–trans* conformation of the O–CH_2–CH_2–O group in the oligo(oxyethylene) chain.[20] The observation of these bands and the absence of the bands characteristic of the *trans* conformation around the OC–CO bond and of the *gauche* conformation around the CC–OC bond indicate that the oligo(oxyethylene) chain in the relevant compounds assumes the *trans–gauche–trans* conformation for the O–CH_2–CH_2–O group.

The spectra of $C_8E_7C_8$ and $C_8E_8C_8$ show distinctive bands at about 1345 and 960 cm^{-1}, denoted with arrows in Fig. 1, which are not observed in the type-B spectra of $C_6E_mC_6$.[13] The former band is assigned to the kink (CH_2–CH_2–CH_2–CH_2 group of the alkyl chain in the *gauche–trans–gauche′* conformation) and the latter is assigned to the end-*gauche* (terminal CH_3CH_2–CH_2–CH_2 group in the *gauche–trans* conformation).[18,19] The observation of these bands shows that the alkyl chains in $C_8E_7C_8$ and $C_8E_8C_8$ contain conformational defects in the solid state. The unannealed $C_8E_6C_8$ giving the type-B spectrum, on the other hand, does not exhibit the bands of the conformational defects, and the molecular conformation is identified as the β-form.

As described above, the molecular form of $C_8E_7C_8$ and $C_8E_8C_8$ is similar to the β-form, but contains the end-*gauche* and kink defects in the alkyl chain. We will call this molecular form the β′-form. It is suggested that, when the defects in the alkyl chain become heavier and more extensive, the β′-form will be led to structure I (noncrystalline alkyl block and crystalline oligo(oxyethylene) block) defined by Booth and co-workers.[8,9] The molecular forms of $C_8E_mC_8$ (m = 1–8) studied in this work are summarized in Table 1. The results show that the molecular form of this series of homologues transforms from the all-*trans* planar γ-form into the planar/helical/planar β-form or the defect-containing β′-form at a length of the oligo(oxyethylene) chain m = 6. It is important to note that the conformational defects are detected in the alkyl chain, even when studied by using highly pure samples, for longer homologues of $C_8E_mC_8$ and are caused most probably by the restricted crystallization of the alkyl blocks as affected by the predominant and pre-crystallizing oligo(oxyethylene) block in the molecule.

The previous study[16] has indicated that the conformation of the $C_nE_mC_n$ compounds in the solid state is closely related to the length of the oligo(oxyethylene) block relative to the length of the alkyl block in the molecule and that the planar oligo(oxyethylene) structure becomes less stable with increasing fraction of the oligo(oxyethylene) block. Accordingly, the conformational transformation is anticipated for $C_8E_mC_8$ to occur at a value of m larger than 5, at which the transformation occurs for $C_6E_mC_6$.[16] The conformational transformation for $C_8E_mC_8$ actually takes place at m = 6 as expected (Table 1).

4.2. Melting behaviour of $C_8E_mC_8$ and polymorphism of $C_8E_6C_8$

The DSC melting curves of $C_8E_mC_8$ (m = 1–8) measured at a rate of heating of 3.0 K min^{-1} are shown in Fig. 2. It is noted that $C_8E_6C_8$ gave two different DSC curves, one for the unannealed sample solidified from the liquid and the other for the sample annealed at about 275 K for more than 30 min. The DSC curves of $C_8E_mC_8$ except the unannealed $C_8E_6C_8$ are not affected by the rate of heating in a range from 0.3 to 20.0 K min^{-1}. In spite of the fact that the molecular form of $C_8E_1C_8$–$C_8E_5C_8$ and $C_8E_6C_8$ (annealed) is different from that of $C_8E_6C_8$ (unannealed), $C_8E_7C_8$ and $C_8E_8C_8$ (Table 1), the features of the DSC melting curves for all the compounds studied, except $C_8E_6C_8$ (unannealed), resemble one another in appearance. For a series of $C_6E_mC_6$ (m = 1–7) previously studied,[16] on the other hand, a single endothermic peak was observed for the γ-form and two endothermic peaks were observed for the β-form. The DSC curves of the β- and β′-form solid of $C_8E_mC_8$ show no clear endothermic peak assignable to solid–solid transition, while admitting that $C_8E_8C_8$ gives a weak endothermic peak at about 270 K. A closer examination of the DSC curves of $C_8E_5C_8$ and $C_8E_7C_8$ indicates that an additional unresolved weak shoulder is observed at the lower-temperature side of the main peak. Although this shoulder is assignable to a solid–solid transition, we consider the composite peak for these compounds as a single endothermic peak associated with the melting, as we could not separate the shoulder from the main peak even at a slower rate of heating of 0.3 K min^{-1}.

As described above, $C_8E_6C_8$ gives, depending on whether the sample is annealed or unannealed, two different DSC melting curves when heated at a rate of 3.0 K min^{-1} (Fig. 2). While the observed curve of the annealed $C_8E_6C_8$ exhibits a single endothermic peak, the curve of the unannealed $C_8E_6C_8$

Table 1 Molecular forms[a] of $C_8E_mC_8$ (m = 1–8) in the solid state

m = 1	m = 2	m = 3	m = 4	m = 5	m = 6		m = 7	m = 8
					Annealed	Unannealed		
γ	γ	γ	γ	γ	γ	β	β′	β′

[a] For the molecular forms, see Fig. 1 of ref. 16. The β′-form is similar to the β-form, but contains the end-*gauche* and kink defects in the alkyl chain.

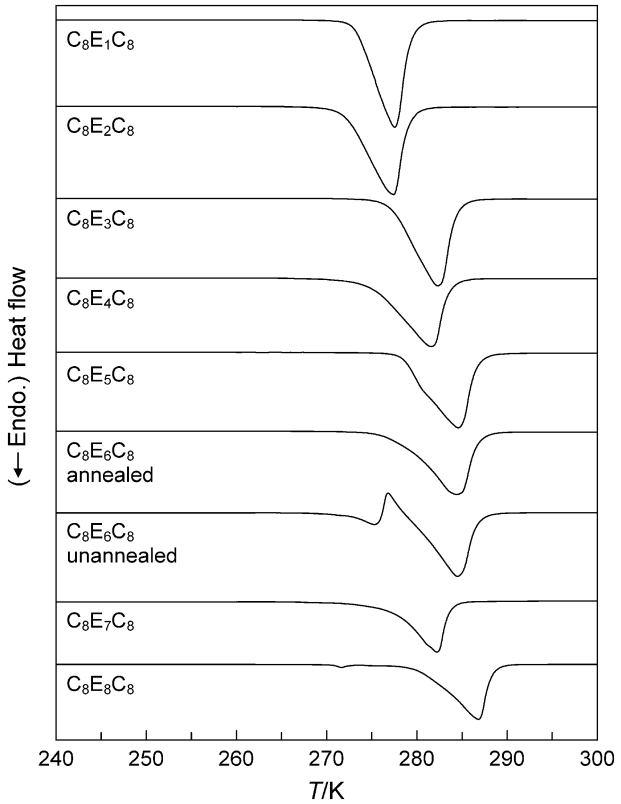

Fig. 2 DSC melting curves of $C_8E_mC_8$ (m = 1–8) measured at a rate of heating of 3.0 K min^{-1}.

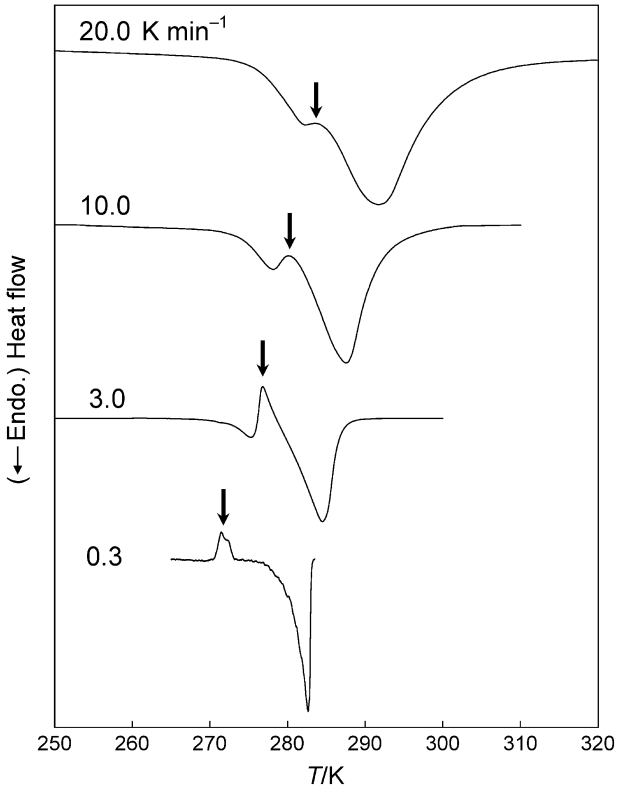

Fig. 3 DSC melting curves of the unannealed $C_8E_6C_8$ measured at different rates of heating (0.3, 3.0, 10.0 and 20.0 K min^{-1}). The arrow indicates the position of an exothermic peak.

exhibits an exothermic peak overlapped partly with the endothermic peak. The two thermal-history-dependent DSC curves of $C_8E_6C_8$ correlate well with the two molecular forms, *i.e.*, the γ-form (annealed) and the β-form (unannealed). The DSC melting curve of the unannealed $C_8E_6C_8$ varies with the change of the rate of heating as shown in Fig. 3. It is noted that the exothermic peak, denoted by an arrow in the figure, together with the endothermic peak moves to lower temperature with a decrease of the rate of heating. This observation indicates that a monotropic solid–solid phase transition takes place during the DSC measurements from the metastable β-form solid to the stable γ-form solid on heating of the unannealed sample.

The thermodynamic quantities of $C_8E_mC_8$ (m = 1–8) derived from the DSC melting curves measured at a rate of heating of 3.0 K min^{-1} are listed in Table 2 where the melting point or the transition temperature is taken at an extrapolated onset of the relevant DSC peak, and the entropy of melting (or transition) is given as the enthalpy of melting (transition) divided by the melting point (transition temperature). The dependencies on the relative molecular mass (M_r) of the melting point (T_m) and the solid–solid transition temperature (T_t) of $C_8E_mC_8$ are shown in Fig. 4, where T_m of $C_6E_mC_6$[16] and the melting point of the rotator phase ($T_{m(ro)}$) and the crystalline–rotator phase transition temperature ($T_{t(cry-ro)}$) of *n*-alkanes[22–24] are also shown for comparison. Note that, although *n*-$C_{16}H_{34}$ (M_r 226.4), *n*-$C_{18}H_{38}$ (M_r 254.5) and *n*-$C_{20}H_{42}$ (M_r 282.5) do not experience the rotator phase before melting unlike other *n*-alkanes used for comparison, we will still use, for the sake of convenience, the notation of $T_{m(ro)}$ to mean their melting point in Fig. 4. Similar convenience will also be applied to the enthalpy of melting and the entropy of melting of these *n*-alkanes in the two subsequent figures.

Fig. 5 shows the dependencies on M_r of the enthalpy of melting (ΔH_m) and the enthalpy of solid–solid transition (ΔH_t)

Table 2 Thermodynamic quantities[a] of $C_8E_mC_8$ (m = 1–8)

Compound	T_m[b]/K	ΔH_m/kJ mol^{-1}	ΔS_m[c]/J K^{-1} mol^{-1}	T_t[b]/K	ΔH_t/kJ mol^{-1}	ΔS_t[d]/J K^{-1} mol^{-1}
γ-Form (all-*trans* planar form)						
$C_8E_1C_8$	276.0	57.11(0.12)	206.9(0.5)	—	—	—
$C_8E_2C_8$	274.9	60.69(0.14)	220.8(0.6)	—	—	—
$C_8E_3C_8$	279.5	71.32(0.09)	255.1(0.3)	—	—	—
$C_8E_4C_8$	277.4	74.59(0.14)	268.9(0.6)	—	—	—
$C_8E_5C_8$	281.0	84.39(0.06)	300.4(0.2)	—	—	—
$C_8E_6C_8$ (annealed)	280.7(0.1)	88.50(0.10)	315.3(0.5)	—	—	—
β- or β′-Form (planar/helical/planar form)						
$C_8E_6C_8$ (unannealed) (β-form)	—	—	—	273.9	—	—
$C_8E_7C_8$ (β′-form)	279.8	77.44(0.82)	276.8(2.9)	—	—	—
$C_8E_8C_8$ (β′-form)	284.3(0.1)	94.13(1.16)	331.1(4.1)	272.6(0.2)	0.99(0.06)	3.6(0.2)

[a] T_m, melting point; ΔH_m, enthalpy of melting; ΔS_m, entropy of melting; T_t, solid–solid transition temperature; ΔH_t, enthalpy of solid–solid transition; ΔS_t, entropy of solid–solid transition. Standard deviations are given in parentheses. [b] Standard deviations less than 0.1 K are not shown. [c] $\Delta S_m = \Delta H_m/T_m$. [d] $\Delta S_t = \Delta H_t/T_t$.

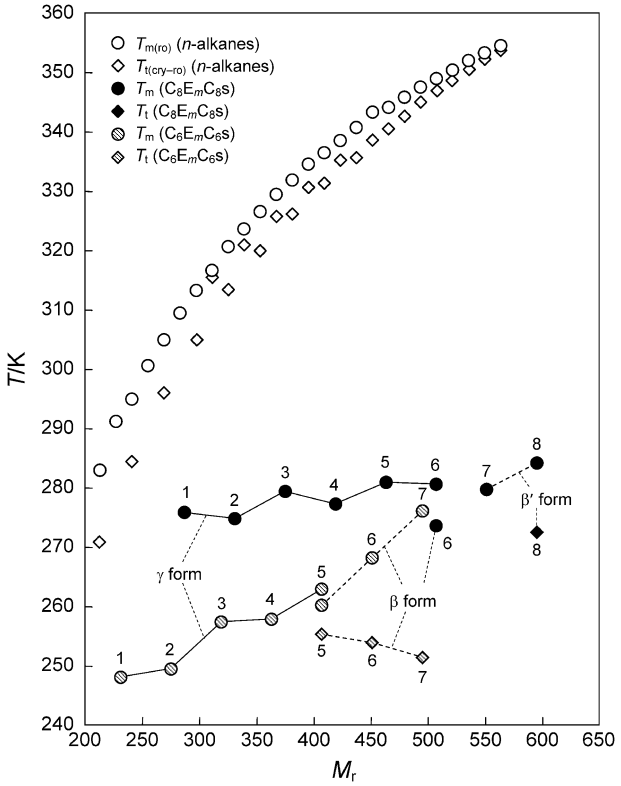

Fig. 4 T_m and T_t of $C_8E_mC_8$ and $C_6E_mC_6$, and $T_{m(ro)}$ and $T_{t(cry-ro)}$ of *n*-alkanes. The number of oxyethylene units (*m*) for $C_8E_mC_8$ and $C_6E_mC_6$ is shown by numerals. The data for $C_6E_mC_6$ are taken from ref. 16 and the data for *n*-alkanes are taken from refs 22–24.

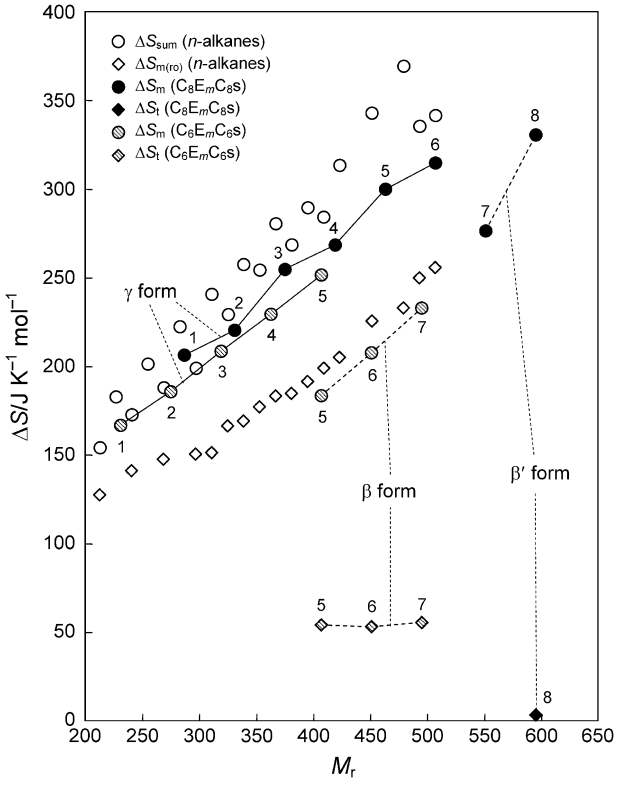

Fig. 6 ΔS_m and ΔS_t of $C_8E_mC_8$ and $C_6E_mC_6$, and ΔS_{sum} and $\Delta S_{m(ro)}$ of *n*-alkanes. The number of oxyethylene units (*m*) for $C_8E_mC_8$ and $C_6E_mC_6$ is shown by numerals. For the references, see the legend to Fig. 4.

of $C_8E_mC_8$ and $C_6E_mC_6$.[16] This figure also presents the pertinent data of *n*-alkanes,[22–24] *i.e.*, the enthalpy of melting of the rotator phase ($\Delta H_{m(ro)}$) and a sum (ΔH_{sum}) of the enthalpy of

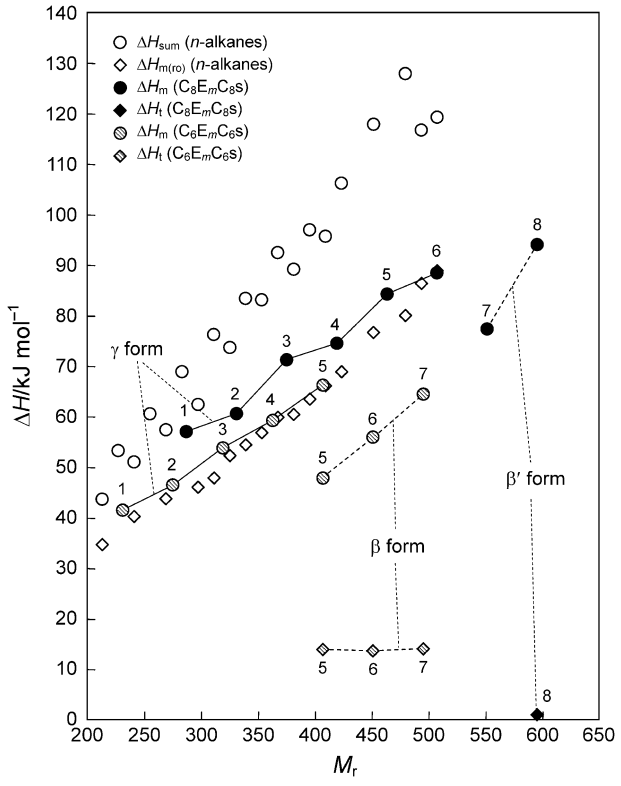

Fig. 5 ΔH_m and ΔH_t of $C_8E_mC_8$ and $C_6E_mC_6$, and ΔH_{sum} and $\Delta H_{m(ro)}$ of *n*-alkanes. The number of oxyethylene units (*m*) for $C_8E_mC_8$ and $C_6E_mC_6$ is shown by numerals. For the references, see the legend to Fig. 4.

crystalline–rotator phase transition ($\Delta H_{t(cry-ro)}$) and $\Delta H_{m(ro)}$. It should be noted that in our analysis we use ΔH_{sum}, rather than $\Delta H_{m(ro)}$, of *n*-alkanes for comparing with ΔH_m of $C_8E_mC_8$ (γ-form) and $C_6E_mC_6$ (γ-form), because the crystalline *n*-alkanes melt *via* the rotator phase. Fig. 6 shows the dependencies on M_r of the entropy of melting (ΔS_m) and the entropy of solid–solid transition (ΔS_t) of $C_8E_mC_8$ and $C_6E_mC_6$,[16] and the entropy of melting of the rotator phase ($\Delta S_{m(ro)}$) and a sum (ΔS_{sum}) of the entropy of crystalline–rotator phase transition ($\Delta S_{t(cry-ro)}$) and $\Delta S_{m(ro)}$ of *n*-alkanes.[22–24]

We will discuss below the melting behaviour of the three solids of $C_8E_mC_8$ (m = 1–8), *i.e.*, the γ-form solid of $C_8E_1C_8$–$C_8E_5C_8$ and $C_8E_6C_8$ (annealed), the β-form solid of $C_8E_6C_8$ (unannealed) and the β′-form solid of $C_8E_7C_8$ and $C_8E_8C_8$.

4.3. Melting of the γ-form solid

In our previous studies on the melting behaviour of the γ-form solid of symmetric $C_nE_mC_n$ compounds,[16,25] we found that the values of T_m for $C_nE_mC_n$ are much lower than the values of $T_{m(ro)}$ for *n*-alkanes with similar values of M_r and that the values of T_m for $C_6E_mC_6$ exhibit the odd–even alternation with respect to the number of oxyethylene units (*m*). As seen from Fig. 4, the γ-form solid of $C_8E_mC_8$ shows the melting behaviour similar to that of $C_6E_mC_6$.[16] The melting points T_m of $C_8E_mC_8$ are higher than those of $C_6E_mC_6$ with similar values of M_r, as explained by the increased fraction of alkyl blocks in the molecule of $C_8E_mC_8$. These observations indicate that the melting behaviour of the γ-form $C_8E_mC_8$ and the γ-form $C_6E_mC_6$ is similar.

Fig. 5 shows that the values of ΔH_m for the γ-form $C_8E_mC_8$ are similar to those for $C_6E_mC_6$, but are considerably smaller than the values of ΔH_{sum} for *n*-alkanes with similar values of M_r. The values of ΔH_m for $C_8E_mC_8$ separate more from the values of ΔH_{sum} with increasing m and come closer to the values of $\Delta H_{m(ro)}$. This tendency of enthalpy changes implies

that the introduction of an oxyethylene unit (OCH_2CH_2) into the molecule reduces the increase of ΔH_m with increasing M_r, as compared with the introduction of the corresponding alkyl unit ($CH_2CH_2CH_2$). At $m = 6$ where the polymorphism is exhibited, the value of ΔH_m coincides substantially with the value of $\Delta H_{m(ro)}$ for *n*-alkane. This behaviour of ΔH_m, which is the same as that observed for $C_6E_mC_6$, can be interpreted by the following factors:[16] (1) an increasing contribution of the conformational restoring force in the oligo(oxyethylene) block in the crystal, resulting from a tendency of the oligo(oxyethylene) chain to resume its intrinsic helical structure; (2) intermolecular local dipole–dipole interactions of the polar C–O bonds; and (3) the presence of a small void between the planar oligo(oxyethylene) chains in the crystal. A conformational transformation from the planar γ-form into the β- or β′-form with helical oligo(oxyethylene) block takes place for $C_8E_mC_8$ at $m = 6$, where the value of ΔH_m coincides with the value of $\Delta H_{m(ro)}$ for the corresponding *n*-alkane. This result, combined with the previous result for $C_6E_mC_6$,[16] demonstrates that the planar structure of the oligo(oxyethylene) chain is stabilized by the force of the magnitude that maintains the rotator phase of *n*-alkanes.

According to the results in Fig. 6, the M_r-dependent behaviour of ΔS_m for the γ-form solid of $C_8E_mC_8$ is substantially the same as that observed for $C_6E_mC_6$.[16] Namely, the values of ΔS_m for $C_8E_mC_8$, which are slightly smaller than the values of ΔS_{sum} for the *n*-alkanes, increase with increasing M_r less rapidly than the values of ΔS_{sum}. We can assume that the entropy of melting ΔS_m is expressed as a sum of the following three terms: (1) change in entropy due to the increase in volume on melting; (2) change in entropy due to the occurrence of long-range disorder including the changes of the position and the orientation of molecules; and (3) change in entropy due to the increased conformational freedom of molecules in the melt.[26–29] On the basis of this assumption, we have interpreted the M_r-dependent behaviour of ΔS_m for $C_6E_mC_6$ to be associated primarily with the second term, namely, the change in entropy due to the occurrence of long-range disorder (ΔS_d).[16] The same interpretation is valid for $C_8E_mC_8$, since this series of homologues shows the same behaviour of ΔS_m as $C_6E_mC_6$. The entropy change ΔS_d is related to the randomness of molecular configurations in the melt. As the local miscibility of the oligo(oxyethylene) block and the alkyl block is low, they tend to separate from one another, resulting in the formation of their domains in the melt with structural organization, like the microdomain structure of block copolymers.[30] Accordingly, the increase of the fraction of the oligo(oxyethylene) block in the $C_nE_mC_n$ molecule should promote the formation of organized structure in the melt. This makes the value of ΔS_d small and eventually results in lowing ΔS_m.

4.4. Melting of the β-form solid

In a previous work,[16] we found that the DSC melting curves of the β-form $C_6E_mC_6$ have two main endotherms corresponding to the melting of the alkyl blocks at T_t and the melting of the oligo(oxyethylene) block at T_m. This observation indicates that the β-form solid of $C_6E_mC_6$ melts stepwise *via* a partially melted structure in a temperature range between T_t and T_m. The β-form solid of $C_8E_6C_8$ (unannealed), on the other hand, melts *via* the γ-form solid, as described above, even with a high rate of heating of 20.0 K min^{-1}. The rapid transition from the β-form to the γ-form did not allow us to measure thermodynamic quantities of the β-form solid of $C_8E_6C_8$.

4.5. Melting of the β′-form solid

We have found in this work a distinctive molecular form, the β′-form, for $C_8E_7C_8$ and $C_8E_8C_8$, for which the conformational defects are involved in the alkyl blocks. The infrared spectral observations indicate that the β′-form is retained down to a low temperature of 100 K, irrespective of thermal treatment. This suggests that the conformational defects (end-*gauche* and kink) in the alkyl chain are intrinsic to the β′-form of the $C_8E_7C_8$ and $C_8E_8C_8$ solid. The involvement of the conformational defects implies that the alkyl blocks of the β′-form are partially noncrystalline.

In the melting process of the β-form solid of $C_6E_mC_6$, the solid–solid transition due to the melting of the alkyl blocks takes place before the melting of the oligo(oxyethylene) block.[16] At this transition, a distinct endotherm was observed in the DSC measurements. For the β′-form solid of $C_8E_mC_8$ in this work, no distinct endotherm associated with the melting of the alkyl blocks was observed (Fig. 2). This thermal behaviour of the β′-form solid suggests that the alkyl blocks, which are partially noncrystalline, and the oligo(oxyethylene) block melt together at the melting point T_m, unlike the β-form solid of $C_6E_mC_6$, for which the alkyl blocks melt at T_t and the oligo(oxyethylene) block melts at T_m.[16]

The enthalpy of melting, ΔH_m, of the β′-form solid can be evaluated by using the data of crystalline poly(oxyethylene) on the assumption that the enthalpy of melting of the β′-form solid is associated exclusively with the melting of the helical oligo(oxyethylene) block. The enthalpy of melting of crystalline poly(oxyethylene) (ΔH_m(POE)) is given, in units of kJ (mol of $OCH_2CH_2)^{-1}$, by the equation.[31]

$$\Delta H_m(\mathrm{POE}) = -8.418 + (8.94 \times 10^{-2})T_m - (1.113 \times 10^{-4})T_m^2$$

Using this equation, we obtain the values of ΔH_m (melting of the oligo(oxyethylene) block) for the β′-form solid of $C_8E_7C_8$ and $C_8E_8C_8$ as 55.18 and 64.02 kJ mol^{-1}, respectively. The observed values for these compounds are 77.44 and 94.13 kJ mol^{-1}, respectively (Table 2), which are *ca.* 40–50% larger than the calculated values of ΔH_m. The excess over the calculated values demonstrates that the observed values of ΔH_m for the β′-form solid have the contributions not only from the melting of the oligo(oxyethylene) block, but also from the melting of the alkyl blocks.

The melting behaviour of the β′-form solid of $C_8E_mC_8$ can also be discussed on the basis of the entropy of melting. In a previous study on the β-form solid of $C_6E_mC_6$,[16] we found that the increment of ΔS_m with an increase of the oxyethylene unit *m* almost coincides with that for completely crystalline poly(oxyethylene) (24.4 J K^{-1} (mol of $OCH_2CH_2)^{-1}$).[32] This implies that the melting of the β-form solid involves only the melting of oligo(oxyethylene) block. For the β′-form solid, the increment of ΔS_m from $C_8E_7C_8$ to $C_8E_8C_8$ is 54.3 J K^{-1} (mol of $OCH_2CH_2)^{-1}$, which is significantly larger than the value for crystalline poly(oxyethylene). This consequence indicates that the melting of the β′-form solid involves the melting of the alkyl blocks as well as the melting of the oligo(oxyethylene) block. The missing observation of an endotherm on the DSC melting curve is consistent with the melting behaviour of the β′-form solid, as discussed above.

5. Conclusions

The present study has clarified the chain-length-dependent conformational transformation and the melting behaviour of the $C_8E_mC_8$ triblock compounds (m = 1–8). The compounds with m = 1–5 assume the all-*trans* planar form (γ-form) in the solid state, while those with m = 7 and 8 assume the planar/helical/planar form with conformational defects in the alkyl chain (β′-form). Conformational polymorphism was observed for $C_8E_6C_8$: the γ-form for the annealed solid and the planar/helical/planar form without conformational defects (β-form) for the unannealed solid. The conformational transformation from the planar form into the planar/helical/planar form takes place at a length of the oligo(oxyethylene) chain $m = 6$. This result for $C_8E_mC_8$ and a similar conformational

transformation for $C_6E_mC_6$ at $m = 5$ (previous work) demonstrate that the conformation of the $C_nE_mC_n$ triblock compounds in the solid state is determined by intramolecular conformational restoring force in the central oligo(oxyethylene) block, intermolecular dipole–dipole interaction of the C–O bonds and intermolecular packing force in the end alkyl blocks.

The melting points of the γ-form solid of $C_8E_mC_8$ are much lower than the melting points of *n*-alkanes with similar molecular masses. The observed thermodynamic quantities show that the planar structure of the oligo(oxyethylene) chain is stabilized by the force of the magnitude that maintains the rotator phase of *n*-alkanes. For the β′-form solid of $C_8E_mC_8$, the alkyl blocks, which are partially noncrystalline, and the oligo(oxyethylene) block melt together at the melting point, unlike the β-form solid of $C_6E_mC_6$, for which the melting of the alkyl blocks takes place before the melting of the oligo (oxyethylene) block. The β-form solid of $C_8E_6C_8$ (unannealed) melts *via* the γ-form solid.

Acknowledgements

This work was partially supported by a Grant-in-Aid for Scientific Research (13640513) from the Ministry of Education, Culture, Sports, Science and Technology of Japan. Kyriakos Viras thanks the Japan Society for the promotion of science as Invitation Fellowship (S03104).

References

1 L. Mandelkern, *Crystallization of Polymers*, Cambridge University Press, Cambridge, 2nd edn., 2004, **vol. 2**.
2 R. Séguéla and J. Prud'homme, *Polymer*, 1989, **30**, 1446–1455.
3 R. E. Cohen, P.-L. Cheng, K. Douzinas, P. Kofinas and C. V. Berney, *Macromolecules*, 1990, **23**, 324–327.
4 K. C. Douzinas, R. E. Cohen and A. F. Halasa, *Macromolecules*, 1991, **24**, 4457–4459.
5 S. Nojima, K. Kato, S. Yamamoto and T. Ashida, *Macromolecules*, 1992, **25**, 2237–2242.
6 C. W. Bunn, *Trans. Faraday Soc*., 1939, **35**, 482–491.
7 Y. Takahashi and H. Tadokoro, *Macromolecules*, 1973, **6**, 672–675.
8 R. C. Domszy and C. Booth, *Makromol. Chem*., 1982, **183**, 1051–1070.
9 H. H. Teo, T. G. E. Swales, R. C. Domszy, F. Heatley and C. Booth, *Makromol. Chem*., 1983, **184**, 861–877.
10 H. Matsuura, K. Fukuhara and O. Hiraoka, *J. Mol. Struct*., 1988, **189**, 249–256.
11 K. Fukuhara, T. Sagawa, S. Kihara and H. Matsuura, *J. Mol. Struct*., 1996, **379**, 197–204.
12 K. Fukuhara, F. Sakogawa and H. Matsuura, *J. Mol. Struct*., 1997, **405**, 123–131.
13 K. Fukuhara, K. Hashiwata, K. Takayama and H. Matsuura, *J. Mol. Struct*., 2000, **523**, 269–280.
14 K. Fukuhara, S. Masatoki, T. Yonemitsu and H. Matsuura, *J. Mol. Struct*., 1998, **444**, 69–76.
15 Y. Chen, G. L. Baker, Y. Ding and J. F. Rabolt, *J. Am. Chem. Soc*., 1999, **121**, 6962–6963.
16 K. Fukuhara, T. Mizawa, T. Inoue, H. Kumamoto and H. Matsuura, *J. Phys. Chem. B*, 2004, **108**, 515–522.
17 T. Gibson, *J. Org. Chem*., 1980, **45**, 1095–1098.
18 G. Zerbi, R. Magni, M. Gussoni, K. Holland-Moritz, A. Bigotto and S. Dirlikov, *J. Chem. Phys*., 1981, **75**, 3175–3194.
19 M. Maroncelli, S. P. Qi, H. L. Strauss and R. G. Snyder, *J. Am. Chem. Soc*., 1982, **104**, 6237–6247.
20 H. Matsuura and K. Fukuhara, *J. Polym. Sci., Part B: Polym. Phys*., 1986, **24**, 1383–1400.
21 H. Matsuura, *Comput. Chem*., 1990, **14**, 59–67.
22 M. G. Broadhurst, *J. Res. Natl. Bur. Stand., Sect. A*, 1962, **66**, 241–249.
23 E. S. Domalski and E. D. Hearing, *J. Phys. Chem. Ref. Data*, 1996, **25**, 1–523.
24 *CRC Handbook of Chemistry and Physics*, ed. D. R. Lide, CRC Press, Boca Raton, FL, 82nd edn., 2001, pp. 6-135–6-136.
25 K. Fukuhara, M. Akisue and H. Matsuura, *Chem. Lett*., 2001, **30**, 828–829.
26 H. W. Starkweather, Jr. and R. H. Boyd, *J. Phys. Chem*., 1960, **64**, 410–414.
27 A. Bondi, *Chem. Rev*., 1967, **67**, 565–580.
28 A. Turturro and U. Bianchi, *J. Chem. Phys*., 1975, **62**, 1668–1673.
29 S. H. Yalkowsky, *Ind. Eng. Chem. Fundam*., 1979, **18**, 108–111.
30 G. E. Molau, in *Block Polymers*, ed. S. L. Aggarwal, Plenum, New York, 1970, pp. 79–106.
31 C. Campbell, K. Viras, M. J. Richardson, A. J. Masters and C. Booth, *Makromol. Chem*., 1993, **194**, 799–816.
32 L. Mandelkern, *J. Appl. Phys*., 1955, **26**, 443–451.